

Space-time vortex driven crossover and vortex turbulence in one-dimensional driven open condensates

Liang He^{1,2}, Lukas M. Sieberer^{3,4} and Sebastian Diehl^{1,2}

¹*Institute for Theoretical Physics, Technical University Dresden, D-01062 Dresden, Germany*

²*Institute for Theoretical Physics, University of Cologne, D-50937 Cologne, Germany*

³*Department of Condensed Matter Physics, Weizmann Institute of Science, Rehovot 7610001, Israel and*

⁴*Department of Physics, University of California, Berkeley, California 94720, USA*

We find a first order transition driven by the strength of non-equilibrium conditions of one-dimensional driven open condensates. Associated with this transition is a new stable non-equilibrium phase, space-time vortex turbulence, whose vortex density and quasiparticle distribution show strongly non-thermal behavior. Below the transition, we identify a new time scale associated with noise activated unbound space-time vortices, beyond which the temporal coherence function changes from a Kardar-Parisi-Zhang type subexponential to a disordered exponential decay. Experimental realization of the non-equilibrium vortex turbulent phase is facilitated in driven open condensates with a large diffusion rate.

The last decade has witnessed a fast experimental development in realizing driven open quantum systems with many degrees of freedom in different physical setups, for instance, exciton-polariton systems in semiconductor heterostructures [1–3], ultracold atoms [4–6], trapped ions [7, 8], or microcavity arrays [9, 10]. The common characteristic is an explicit breaking of detailed balance on a microscopic level by the presence of coherent and driven-dissipative dynamics on an equal footing, placing these systems far from thermal equilibrium. This makes them promising laboratories for the study of non-equilibrium statistical mechanics, according to which one expects intrinsic non-equilibrium features to persist to the macroscopic level of observation.

A case in point are exciton-polariton systems, which can be engineered in one- and two-dimensional geometries [1–3, 11]. Due to effectively incoherent pumping, these systems possess a phase rotation symmetry and can thus show spontaneous Bose condensation phenomena at sufficiently low noise level. While their dynamics is described microscopically in terms of a stochastic driven-dissipative Gross-Pitaevski equation [12], recently it was noticed that at low frequencies the dynamics can be mapped onto the Kardar-Parisi-Zhang (KPZ) equation [13]. Traditionally, the latter equation describes, e.g., the roughening of surfaces, with the dynamical surface height being unconstrained [14]. In contrast, the dynamical variable in the context of driven open quantum systems is the condensate phase, which is compact. The compact KPZ equation (cKPZ) gives rise to a novel scenario for non-equilibrium statistical mechanics realized in concrete experimental platforms, and raises the fundamental question of the physical consequences of compactness.

In this work, we address this question for one-dimensional driven open quantum systems. To this end, we establish the complete phase diagram of 1D driven open condensates (DOC) via numerical simulations in combination with analytic analysis, and explain its basic structure on the basis of the 1D cKPZ equation (cf. Fig. 1). It can be traced back to the behavior of dynamical topological defects, namely space-time vortices (Fig. 1 (b)). More specifically, we find: (i) The emergence of a new time scale t_v in the long time behavior of the temporal coherence function. At weak noise level σ , it is exponentially large, $t_v \sim e^{B/\sigma}$ (B a non-universal positive constant), reflecting an exponentially suppressed but finite space-time vortex density (Fig. 1

(c)). The subsequent asymptotic scaling regime $t \gg t_v$ is characterized by a disordered, exponentially decaying first order temporal coherence function. The exponential dependence on the inverse noise level corroborates previous results on the observability of KPZ physics in 1D, where the crossover scale from stretched exponential equilibrium diffusive to non-equilibrium KPZ scaling behaves algebraically as $t_* \sim \sigma^{-2}$ [15] at weak noise level, ensuring generically $t_* \ll t_v$. Interestingly, this relation is reversed in the context of two-dimensional driven open quantum systems, where recently a relation $t_v \ll t_*$ (or for the related length scales $L_v \ll L_*$) was established, with *both* scales being exponentially large in the microscopic parameters [16, 17]. (ii) We identify a new intrinsic non-equilibrium phase of the cKPZ equation, with the following key signatures: (a) A first order transition at low noise level from a regime of exponentially low to high space-time vortex density (cf. Fig. 1 (d)). (b) A strongly non-thermal behavior of the momentum distribution of quasiparticles $n_q \sim q^{-\gamma}$ at large momentum q (cf. Fig. 3), with γ significantly deviating from the value for thermal behavior ($\gamma \sim 2$). The occupation number is accessible in exciton-polariton systems via momentum resolved correlation measurements [12]. Such a strong scaling behavior is reminiscent of turbulence, which usually is a transient phenomenon that occurs in specifically initialized systems undergoing purely Hamiltonian dynamics without external drive [18]. In contrast, it occurs in stationary state in our case.

Microscopic model.— We describe the dynamics in terms of the stochastic driven-dissipative Gross-Pitaevski (or stochastic complex Ginzburg-Landau (SCGLE)) equation with a complex Gaussian white noise (units $\hbar = 1$) of zero mean, as appropriate for experiments with exciton-polariton systems [1–3]. It reads in 1D [12]

$$\frac{\partial}{\partial t} \psi = \left[r + K \frac{\partial^2}{\partial x^2} + u |\psi|^2 \right] \psi + \zeta, \quad (1)$$

with $r = r_d + i r_c$, $K = K_d + i K_c$, $u = -u_d - i u_c$, $\langle \zeta(x, t) \zeta(x', t') \rangle = 0$, $\langle \zeta^*(x, t) \zeta(x', t') \rangle = 2\sigma \delta(x - x') \delta(t - t')$. r_c and u_c are the chemical potential and the elastic collision strength, respectively. $r_d = \gamma_p - \gamma$ is the difference between the single particle loss γ_l and incoherent pump γ_p . For the existence of a condensate in the mean field steady state solution, $r_d > 0$ with the single-particle pump outweighing the loss rate. u_d is the positive two-particle loss rate; $K_c = 1/(2m_{LP})$ with m_{LP} the effective

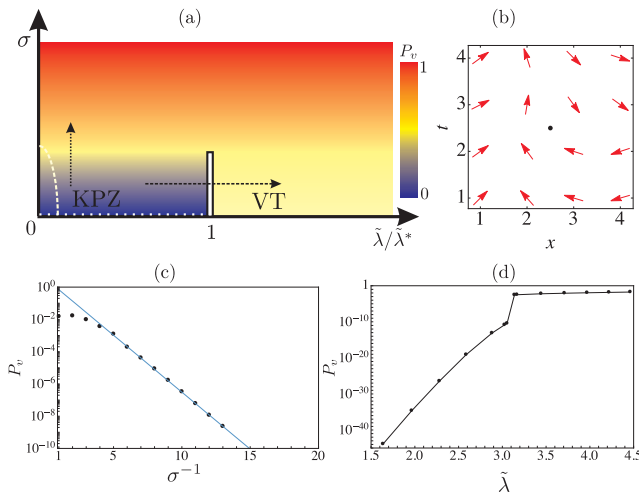


Figure 1: (Color online) (a) Schematic phase diagram of a generic 1D driven open condensate (DOC) with noise level σ and rescaled non-equilibrium strength parameter $\tilde{\lambda}/\tilde{\lambda}^*$. The color code stands for space-time vortex density P_v . A first order phase transition at low noise level separates a regime dominated by KPZ physics from a vortex turbulent (VT) regime. Current exciton-polariton condensate experiments are located within the white dashed arc. At $\sigma = 0$ and $\tilde{\lambda}/\tilde{\lambda}^* < 1$ (white dotted line), the system is in a vortex free state. It is unstable against the creation of free vortices at infinitesimal noise, however with exponentially small corrections (see (c)). (b) A typical phase configuration on the space-time plane corresponding to a phase-slip event at a time point between $t = 2$ and 3. A space-time vortex core is marked with a black dot. (c) Noise level dependence of the space-time vortex density P_v at small non-equilibrium strength $\tilde{\lambda} < \tilde{\lambda}^*$ (vertical dashed arrow in (a)). At low noise level, $P_v \sim e^{-A/\sigma}$ (A a non-universal positive constant) is suppressed exponentially, reflected by the linear fit for $\sigma^{-1} = 6, \dots, 13$. Values of other parameters used in simulations are $K_d = r_d = u_d = 1, r_c = u_c = 0.1$, and $K_c = 3$. (d) Non-equilibrium strength dependence of P_v at low noise level with $\sigma = 10^{-2}$, demonstrating the first order transition upon increasing non-equilibrium strength $\tilde{\lambda}$ (horizontal dashed arrow in (a)). Values of other parameters used in simulations are $K_d = r_d = u_d = 1, K_c = 0.1$, and $r_c = u_c$ is tuned from 1.0 to 3.0. The corresponding values of $\tilde{\lambda}$ increase with respect to u_c from 1.6 to 4.5, according to its explicit definition. See text for more details.

polariton mass and K_d a diffusion constant. We obtained most of the numerical results presented in this work by solving Eq. (1) using the same approach as in Ref. [19] and we set $r_d = K_d = 1$; hence, t and x are measured in units of r_d^{-1} and $\sqrt{K_d}$. If not specified otherwise, we used 10^3 stochastic trajectories to perform ensemble averages.

Low frequency effective description.— In the absence of phase defects, the low frequency dynamics of the system is effectively described by the KPZ equation [14] for the phase of the condensate field, $\partial_t \theta = D \partial_x^2 \theta + \frac{\lambda}{2} (\partial_x \theta)^2 + \xi$ [13]. Here D describes phase diffusion, and there is a Gaussian white noise ξ of strength $2\sigma_{\text{KPZ}}$. The non-linearity λ is a direct, single-parameter measure for the deviation from equilibrium conditions, with $\lambda = 0$ in the presence of detailed balance. In order to properly account for the compactness of the phase and to allow for a description of phase defects, we work with a lattice regularized version of the KPZ equation (cKPZ), which can be straightforwardly derived from a spatially discretized

SCGLE on a 1D lattice with spacing Δ_x [20]. It reads

$$\partial_t \theta_i = \sum_{j=i\pm 1} \left[-\bar{D} \sin(\theta_i - \theta_j) + \bar{\lambda} \sin^2\left(\frac{\theta_i - \theta_j}{2}\right) \right] + \bar{\xi}_i, \quad (2)$$

with $\theta_i(t) \equiv \theta(i\Delta_x, t)$, $\bar{\xi}_i(t)$ being Gaussian white noise with $\langle \bar{\xi}_i(t) \bar{\xi}_{i'}(t') \rangle = 2\bar{\sigma}_{\text{KPZ}} \delta(t - t') \delta_{ii'}$, $\bar{D} = D/\Delta_x^2$, $\bar{\lambda} = \lambda/\Delta_x^2$, $\bar{\sigma}_{\text{KPZ}} = \sigma_{\text{KPZ}}/\Delta_x$, where $D = \frac{u_c K_c}{u_d} + K_d$, $\lambda = 2\left(\frac{u_c K_d}{u_d} - K_c\right)$, $\sigma_{\text{KPZ}} = \sigma \frac{u_c^2 + u_d^2}{2r_d u_d}$. The KPZ equation is reproduced upon assuming that phase fluctuations are small, and taking the continuum limit. The crucial difference between the non-compact continuum KPZ and the compact KPZ equation is revealed by the number of independent scales in the problem, which originates from the compactness of the phase. Indeed, by rescaling t, ξ and θ in the continuum case, the number of independent tuning parameters turns out to be *one*, and given by $g \equiv \lambda(\sigma_{\text{KPZ}}/2D^3)^{1/2}$. In contrast, for the cKPZ equation, we can rescale t and ξ_i but *not* the phase field θ_i due to its compactness, resulting in *two* independent tuning parameters. The rescaled equation obtains from Eq. (2) by the replacements $\bar{D} \rightarrow 1, \bar{\lambda} \rightarrow \tilde{\lambda} = \lambda/D, \bar{\sigma} \rightarrow \tilde{\sigma} = \Delta_x \sigma_{\text{KPZ}}/D$. The rescaled equations with $\tilde{\lambda}$ and $-\tilde{\lambda}$ are equivalent, therefore we further redefine $\tilde{\lambda} \equiv |\lambda/D|$. The independence on $\tilde{\lambda}$ and $\tilde{\sigma}$ suggests that there must exist new physics associated with changing each of the two parameters, beyond the physics of the KPZ equation where changing the nonequilibrium strength $\tilde{\lambda}$ and noise strength $\tilde{\sigma}$ are equivalent to changing the single parameter g . Indeed, as we shall see in the following, the noise strength is associated with a new time scale in the 1D DOC giving rise to an additional scaling regime in dynamical correlation functions. Moreover, the non-equilibrium strength $\tilde{\lambda}$ can drive the system to a new non-equilibrium vortex turbulent phase via a first order transition at low noise level.

Space-time vortex driven crossover for $\tilde{\lambda}/\tilde{\lambda}^ < 1$.*— The prime observable that distinguishes a 1D DOC described by Eq. (1) from its equilibrium counterpart [19, 21] is the autocorrelation function $C_t^\psi(x; t_1, t_2) \equiv \langle \psi^*(x, t_1) \psi(x, t_2) \rangle$. Its long time behavior is determined by fluctuations of the phase, $C_t^\psi(x; t_1, t_2) \propto e^{-c\Delta_\theta(t_1 - t_2)}$, where c is a non-universal constant, and [22]

$$\Delta_\theta(t_1 - t_2) \equiv \frac{1}{L} \int_0^L dx \langle [\theta(x, t_1) - \theta(x, t_2)]^2 \rangle - \langle \theta(x, t_1) - \theta(x, t_2) \rangle^2, \quad (3)$$

with L being the spatial size of the system. Previous numerical studies [19, 21] confirmed KPZ scaling $\Delta_\theta(t_1 - t_2) \propto |t_1 - t_2|^{2\beta}$ with $\beta = 1/3$ (in contrast to $\beta = 1/4$ in thermal equilibrium with $\tilde{\lambda} = 0$) *in the regime of weak noise*. The latter is defined by the absence of phase slips—or, equivalently, space-time vortices, see Fig. 1 (b)—in the spatio-temporal extent of the numerical experiments. Increasing the noise level leads to proliferation of phase slips, which in turn strongly affect the temporal coherence of DOCs as we describe in the following.

Figure 2 (a) shows $\Delta_\theta(t_1 - t_2)$ obtained by numerical integration of Eq. (1) for moderate noise strengths. For the lowest value $\sigma = 8^{-1}$, KPZ scaling can be observed

in a wide range $5 \times 10^3 \lesssim |t_1 - t_2| \lesssim 5 \times 10^4$, after which $\Delta_\theta(t_1 - t_2)$ grows linearly with time. Accordingly, the autocorrelation function $C_t^\psi(x; t_1, t_2)$ exhibits a crossover from stretched-exponential to simple exponential decay at long times [20]. At weak noise, the crossover time t_c , which we define as the point where the gradient of $\Delta_\theta(t_1 - t_2)$ on a double logarithmic scale exceeds 0.9, decreases exponentially with the noise level, i.e., $t_c \propto e^{C/\sigma}$, where C is a positive constant. This is shown in Fig. 2 (b).

The fast growth of phase fluctuations and the associated decoherence of DOCs for strong noise and at long times is due to space-time vortices. Numerical evidence for this connection is presented in Fig. 1 (c), which shows the dependence of the space-time vortex density P_v on the noise strength. The linear fit on the semi-logarithmic scale clearly demonstrates that $P_v \propto e^{-A/\sigma}$ in the range $6 \lesssim \sigma^{-1} \lesssim 13$, while saturation sets in at even higher noise strengths. As we explain below, the exponential determining P_v is the same as the one appearing in t_c and can be interpreted as the statistical weight of space-time vortex configurations in an equivalent 1+1D static equilibrium description of the problem. Indeed, the exponentially small but finite space-time vortex density entails a time scale t_v characterizing the average temporal distance between vortices [23]

$$t_v \propto P_v^{-3/5} \propto e^{\frac{3A}{5}\sigma^{-1}}, \text{ if } \sigma \ll 1. \quad (4)$$

Then, using a simple phase random walk we show that phase slips occurring at multiples of t_v lead to linear growth of $\Delta_\theta(t)$ beyond a time scale $t_c = \mathcal{O}(t_v)$.

First, however, let us clarify the origin of the recurring exponential. It can be understood by exploiting the equivalence between the cKPZ equation and a *static* problem in thermal equilibrium in two spatial dimensions [20, 24]. Formally, this equivalence can be established by rewriting the cKPZ equation as a functional integral over space-time configurations of the phase field as $Z = \int \mathcal{D}[\theta] e^{-\mathcal{H}[\theta]/T}$ [20, 24]. In this description, the Boltzmann factor $e^{-\mathcal{H}[\theta]/T}$ determines the probability with which a particular solution $\theta(x, t)$ is encountered in a numerical integration of Eq. (2) from time t_0 to t_1 in a system of size L . The temperature is $T = 4\sigma_{\text{KPZ}}$, and the effective Hamiltonian (going back to a spatial continuum notation) is given by

$$\mathcal{H}[\theta] = \int_{t_0}^{t_1} dt \int_0^L dx \left[\partial_t \theta - D \partial_x^2 \theta - \frac{\lambda}{2} (\partial_x \theta)^2 \right]^2. \quad (5)$$

Regarding $z = t$ as a spatial coordinate, this is the Hamiltonian of a 2D smectic A liquid crystal [24]. By definition, a single-vortex configuration $\theta_v(x, t)$ minimizes this Hamiltonian subject to the topological constraint that the circulation of the phase around the location of the vortex core is an integer multiple of 2π . In Ref. [25], the energy $E_v = \mathcal{H}[\theta_v]$ was shown to be finite for $\lambda = 0$. When $\lambda \neq 0$, it is not possible to find $\theta_v(x, t)$ minimizing the energy analytically, but an upper bound on E_v can be obtained by calculating $\mathcal{H}[\theta_v]$ with the $\lambda = 0$ vortex configuration. Crucially, a straightforward integration shows that this upper bound is *finite* [26], indicating that at any finite noise strength there is a non-zero density of thermally excited vortices $P_v \propto e^{-E_v/T}$. Deviations from this exponential dependence in Fig. 1 (c) for strong noise are

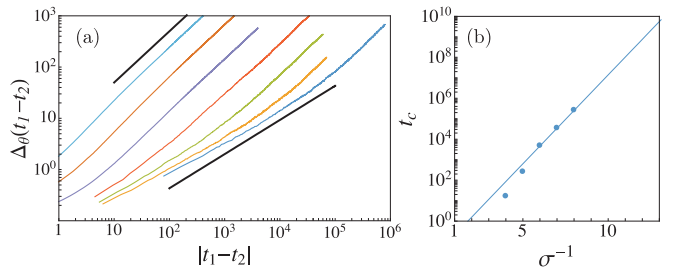


Figure 2: (Color online) (a) Temporal phase fluctuations $\Delta_\theta(t_1 - t_2)$ for different noise levels on a double-logarithmic scale. The upper and lower black solid lines correspond to linear, “disordered” scaling $\sim |t_1 - t_2|$ and KPZ scaling $\sim |t_1 - t_2|^{2/3}$, respectively. From left to right, curves in between the two black solid lines are obtained for σ^{-1} from 2 to 8, while the other parameters are $K_d = r_d = u_d = 1$, $r_c = u_c = 0.1$, and $K_c = 3$. For each noise level, the system size L is chosen large enough to make finite size effects negligible. (b) Crossover time scale t_c as a function of inverse noise strength on a semi-logarithmic scale. The straight line is a linear fit to the data points corresponding to the lowest three noise strengths.

due to the interaction energy of vortices, which becomes important at higher densities.

The rate $1/t_v$ at which phase slips occur and hence the vortex density P_v for a system in thermal equilibrium (described by Eq. (1) with $r_c = K_c = u_c = 0$) was determined in the context of narrow superconducting channels in Refs. [27]. Phase slips are fluctuations which reduce the current and thus leads to a finite resistance of the channel. More formally, during a phase slip the system changes its state from one local minimum of the free energy to a neighboring one that differs in current by $2\pi/L$. At low noise (set by the temperature T), the rate at which such fluctuations occur is proportional to $\exp(-\delta F/T)$ where δF is the height of the free energy barrier separating the local minima. Out of thermal equilibrium, however, the notion of a free energy becomes void and the theory developed in Refs. [27] cannot be applied directly. Then, the approach presented above is a novel viable alternative to obtain the exponential factor.

Having established that the density of space-time vortices is always finite, it remains to verify that they are indeed the cause of the exponential decay of the autocorrelation function. This can be understood by considering a simple “phase random walk” model in which the time evolution of the phase is assumed to be only determined by the phase jumps due to N uniformly distributed vortex cores at times nt_v , where $n = 1, \dots, N$, with random charges $W_n = \pm 1$ occurring with equal probability. The model can be formulated as

$$\theta(x, t_1 + Nt_v) - \theta(x, t_1) = \delta\Theta \sum_{n=1}^N W_n, \quad (6)$$

where $\delta\Theta$ corresponds to the average amplitude of jumps of the phase field if a vortex core is crossed along the temporal direction. A straightforward calculation shows that $\Delta_\theta(t_1 - t_2) = (\delta\Theta)^2 |t_1 - t_2|/t_v$, i.e., space-time vortices indeed lead to disordered behavior of the phase correlations beyond a time scale $\mathcal{O}(t_v)$.

First order transition and vortex turbulence for $\tilde{\lambda}/\tilde{\lambda}^ > 1$.*— We now investigate the strongly non-equilibrium

regime at large $\tilde{\lambda}$. Figure 1 (d) shows the dependence of the vortex density P_v on $\tilde{\lambda}$ at weak noise. At small $\tilde{\lambda}$, P_v is exponentially small in line with the discussion above. However, when tuning above a critical strength $\lambda^* \simeq 3.1$, the vortex density undergoes a sudden jump by around 10 orders of magnitude, indicating a sharp first order transition at low noise level. We emphasize that P_v is finite on both sides of the transition, i.e., the long-time decay of the autocorrelation function is exponential on both sides. The phases are distinct by the density of vortices—similar to the liquid-gas transition in thermal equilibrium.

Above the transition, the system exhibits distinct features in the momentum distribution $n_q \equiv \langle \psi^*(q) \psi(q) \rangle$ (cf. Fig. 3): n_q shows scaling behavior at large q , i.e., $n_q \propto q^{-\gamma}$ with γ being some positive exponent. Below the transition, the value $\gamma \simeq 2$, which is a characteristic for thermally excited uncorrelated vortices [18]. In contrast, above the transition, γ shows significant deviation from the value for thermal vortices. Such strong scaling behavior is reminiscent of turbulence and we thus refer to this phase as vortex turbulence (VT). For the choice of parameters in Fig. 3, $\gamma \simeq 5$ in VT, but it shows a weak parameter dependence. As can be seen in the main plot of Fig. 3, the exponent γ also undergoes a jump across the transition. Thus, the momentum distribution function, which is accessible in experiments with exciton-polaritons, displays clear signatures of the transition.

The physical origin of the VT phase and the associated first order transition can be traced back to a dynamical instability triggered by the nonequilibrium strength above a critical value. To this end, we consider the dynamical equations for the phase *differences* between nearest neighboring sites, $\Delta_i \equiv \theta_i - \theta_{i+1}$, at zero noise level, which assumes the form $\partial_t \Delta_i \simeq -(2\Delta_i - \Delta_{i+1} - \Delta_{i-1}) + \tilde{\lambda}(\Delta_{i-1}^2 - \Delta_{i+1}^2)/4$ when Δ_i is small. The first term on the right hand side, originating from the phase diffusion term in the cKPZ, is a restoring term which attenuates phase differences, while the second term significantly amplifies it for $\tilde{\lambda} \gg 1$ even for small spatial variations. This causes the dynamical instability and gives rise to creation of vortices without resorting to "thermal excitations". Taking into account the exponential suppression of thermally excited vortices at low noise level, and the fact that the vortex generation due to the dynamical instability is insensitive to weak noise, this rationalizes the existence of a first order transition tuned by $\tilde{\lambda}$ and witnessed by the vortex density in steady state. At stronger noise, the first order transition behavior is expected to be smeared out by thermal vortices as indicated in Fig. 1 (a).

The discussion of the VT transition reveals it to be rooted in the physics of the cKPZ equation, and more precisely, to in its driven non-equilibrium nature. Numerically solving this equation at low noise level, we obtain $\tilde{\lambda}^* \simeq 20$ for the critical non-equilibrium strength. This can be compared to the numerical simulations of the SCGLE at weak noise, which yields the significantly reduced value $\tilde{\lambda}^* \simeq 3.1$. The discrepancy is due to the mutual feedback between density and phase fluctuations: phase fluctuations can cause a local density depression via a phase-density coupling term proportional to the diffusion constant K_d (cf. Eq. (1)), which in turn facilitates strong phase fluctuations and gives rise to vortex cre-

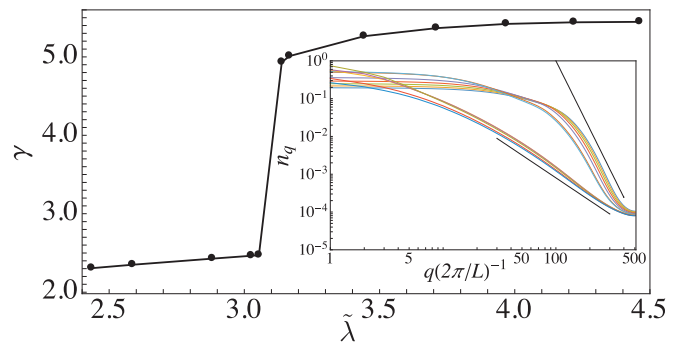


Figure 3: (Color online) Scaling behavior of the momentum distribution $n_q \propto q^{-\gamma}$ at different $\tilde{\lambda}$, revealing the first order transition from a power law $\propto q^{-2}$ to $\propto q^{-5}$. Inset: Momentum distributions from which the power law is extracted. The upper and lower black lines correspond to the power laws $\propto q^{-5}$ and $\propto q^{-2}$, respectively. From right to left, the curves in between the two black lines correspond to $r_c = u_c$ decreasing from 3.0 to 1.5, respectively. The other parameters are the same as in Fig. 1 (d). See text for more details.

ation. Therefore, the critical value $\tilde{\lambda}^*$ in the SCGLE also depends on K_d . We note that dynamical instabilities associated with certain special classes of solutions of the *deterministic* complex Ginzburg-Landau equation were identified in the context of nonlinear dynamics [28]. Our investigation indicates that this dynamical instability is generic and originates from the intrinsic non-equilibrium nature of the problem.

Indications on experimental observations.— Our theoretical investigations above provide two important indications for future experiments with 1D DOCs. In particular, there are two types of experiments, which favor observability of different regimes in the phase diagram Fig. 1. In typical setups [11], the effective inverse polariton mass $K_c = 1/2m_{LP} \gg K_d$, K_d the diffusion constant (cf. Eq. (1)). Such systems suggest observability of KPZ physics, which remains intact in line with previous results [19, 21] at low noise and weak non-equilibrium strength, due to the exponential suppression of unbound vortices in this regime. On the other hand, recently realized experimental setups demonstrating exciton-polariton condensation in the flat band of a 1D Lieb lattice of micropillar optical cavities [29] are promising candidates for the observation of the vortex turbulent phase, whose distinct features in the momentum distribution are directly accessible in DOC systems with momentum resolved correlation measurements [12]. In these systems, the dispersion is suppressed, i.e., $K_c \simeq 0$. In this case, the system's largest achievable nonequilibrium strength is $\tilde{\lambda}_{\max} \sim 2K_d/K_c$, indicating the system can be tuned above the critical strength $\tilde{\lambda}^*$ to trigger the vortex turbulence phase. Alternatively, explicit engineering of a large diffusion constant could be achieved in 1D arrays of microwave resonators coupled to superconducting qubits [30].

Conclusions.— The non-equilibrium phase diagram of one-dimensional driven open condensates is crucially impacted on by space-time vortices, as the relation to the compact KPZ equation reveals: at weak non-equilibrium strength, they govern the asymptotic behavior of the temporal correlation functions, however only beyond an exponentially large crossover time scale. This protects KPZ

physics and suggests its observability in current exciton-polariton experiments. Moreover, these defects cause the existence of a new phase under strong non-equilibrium conditions, stationary vortex turbulence. We believe that our predictions will stimulate both further theoretical research on the cKPZ equation, especially in higher dimensions and in the context of stationary turbulence, as well as experimental efforts in searching for these two non-equilibrium phases. Another intriguing direction for future research is to study nucleation dynamics and phase coexistence in the vicinity of the transition to VT, as well as the nature of the endpoint of the critical line in Fig. 1 (a).

Note added.— Upon completion of this manuscript, we

became aware of the work by R. Lauter, A. Mitra and F. Marquardt reporting a related dynamical instability in arrays of coupled phase oscillators [31].

Acknowledgments— We thank I. Carusotto, B. Kim, E. Altman, D. Huse, J. Toner and S. Mathey for useful discussions and the Center for Information Services and High Performance Computing (ZIH) at TU Dresden for allocation of computer time. This work was supported by German Research Foundation (DFG) through ZUK 64, through the Institutional Strategy of the University of Cologne within the German Excellence Initiative (ZUK 81) and by the European Research Council via ERC Grant Agreement n. 647434 (DOQS).

[1] J. Kasprzak, M. Richard, S. Kundermann, A. Baas, P. Jeambrun, J. M. J. Keeling, F. M. Marchetti, M. H. Szymańska, R. Andre, J. L. Staehli, V. Savona, P. B. Littlewood, B. Deveaud, and L. S. Dang, *Nature* **443**, 409 (2006).

[2] K. G. Lagoudakis, M. Wouters, M. Richard, A. Baas, I. Carusotto, R. Andre, Le Si Dang, and B. Deveaud-Pleidan, *Nature Physics* **4**, 706 (2008).

[3] G. Roumpos, M. Lohse, W. H. Nitsche, J. Keeling, M. H. Szymańska, P. B. Littlewood, A. Löffler, S. Höfling, L. Worschech, A. Forchel, and Y. Yamamoto, *PNAS* **109**, 6467 (2012).

[4] N. Syassen, D. M. Bauer, M. Lettner, T. Volz, D. Dietze, J. J. García-Ripoll, J. I. Cirac, G. Rempe, and S. Dürr, *Science* **320**, 1329 (2008).

[5] C. Carr, R. Ritter, C. G. Wade, C. S. Adams, and K. J. Weatherill, *Phys. Rev. Lett.* **111**, 113901 (2013).

[6] B. Zhu, B. Gadway, M. Foss-Feig, J. Schachenmayer, M. L. Wall, K. R. A. Hazzard, B. Yan, S. A. Moses, J. P. Covey, D. S. Jin, J. Ye, M. Holland, and A. M. Rey, *Phys. Rev. Lett.* **112**, 070404 (2014).

[7] R. Blatt and C. Roos, *Nat. Phys.* **8**, 277 (2012).

[8] J. W. Britton, B. C. Sawyer, A. C. Keith, C.-C. J. Wang, J. K. Freericks, H. Uys, M. J. Biercuk, and J. J. Bollinger, *Nature* **484**, 489 (2012).

[9] M. Hartmann, F. Brandao, and M. Plenio, *Laser Photonics Rev.* **2**, 527 (2008).

[10] A. A. Houck, H. E. Tureci, and J. Koch, *Nat. Phys.* **8**, 292 (2012).

[11] E. Wertz, A. Amo, D. D. Solnyshkov, L. Ferrier, T. C. H. Liew, D. Sanvitto, P. Senellart, I. Sagnes, A. Lemaître, A. V. Kavokin, G. Malpuech, and J. Bloch, *Phys. Rev. Lett.* **109**, 216404 (2012).

[12] I. Carusotto and C. Ciuti, *Rev. Mod. Phys.* **85**, 299 (2013).

[13] E. Altman, L. M. Sieberer, L. Chen, S. Diehl, and J. Toner, *Phys. Rev. X* **5**, 011017 (2015).

[14] M. Kardar, G. Parisi, and Y.-C. Zhang, *Phys. Rev. Lett.* **56**, 889 (1986).

[15] T. Nattermann and L.-H. Tang, *Phys. Rev. A* **45**, 7156 (1992).

[16] G. Wachtel, L. M. Sieberer, S. Diehl, and E. Altman, arXiv:1604.01042.

[17] L. M. Sieberer, G. Wachtel, E. Altman, and S. Diehl, arXiv:1604.01043.

[18] M. Schmidt, S. Erne, B. Nowak, D. Sexty, and T. Gasenzer, *New J. Phys.* **14**, 075005 (2012).

[19] L. He, L. M. Sieberer, E. Altman, and S. Diehl, *Phys. Rev. B* **92**, 155307 (2015).

[20] See Supplemental Material for technical details and additional figures and calculations.

[21] K. Ji, V. N. Gladilin, and M. Wouters, *Phys. Rev. B* **91**, 045301 (2015).

[22] In the definition of $\Delta_\theta(t_1 - t_2)$, the spatial average over the system size L is taken for convenience and does not affect the universal scaling behavior for large time differences $|t_1 - t_2|$.

[23] The mean temporal and spatial distances between vortices, denoted as t_v and x_v respectively, are given in terms of the vortex density by $t_v x_v = 1/P_v$. Inserting here the relation $t_v \sim x_v^z$ with the dynamical exponent $z = 3/2$, which is valid in the scaling regime of the non-compact KPZ equation, leads to Eq. (4).

[24] L. Golubović and Z.-G. Wang, *Phys. Rev. Lett.* **69**, 2535 (1992); L. Golubović and Z.-G. Wang, *Phys. Rev. E* **49**, 2567 (1994); L. Golubović and Z.-G. Wang, *Phys. Rev. E* **50**, 4265 (1994).

[25] J. Toner and D. R. Nelson, *Phys. Rev. B* **23**, 316 (1981).

[26] This is in sharp contrast to a superfluid in 2D in thermal equilibrium for which the energy of a single vortex diverges logarithmically with system size.

[27] J. S. Langer and V. Ambegaokar, *Phys. Rev.* **164**, 498 (1967); D. E. McCumber and B. I. Halperin, *Phys. Rev. B* **1**, 1054 (1970).

[28] I. S. Aranson and L. Kramer, *Rev. Mod. Phys.* **74**, 99 (2002).

[29] F. Baboux, L. Ge, T. Jacqmin, M. Biondi, E. Galopin, A. Lemaître, L. Le Gratiet, I. Sagnes, S. Schmidt, H. E. Türeci, A. Amo, and J. Bloch, *Phys. Rev. Lett.* **116**, 066402 (2016).

[30] D. Marcos, A. Tomadin, S. Diehl, and P. Rabl, *New J. Phys.* **14**, 055005 (2012); J. Marino and S. Diehl, *Phys. Rev. Lett.* **116**, 070407 (2016); J. Marino and S. Diehl, arXiv:1606.00452.

[31] R. Lauter, A. Mitra, and F. Marquardt, arXiv:1607.03696.

Supplemental Material for “Space-time vortex driven crossover and vortex turbulence in one-dimensional driven open condensates”

Liang He^{1,2}, Lukas M. Sieberer^{3,4} and Sebastian Diehl^{1,2}

¹*Institute for Theoretical Physics, Technical University Dresden, D-01062 Dresden, Germany*

²*Institute for Theoretical Physics, University of Cologne, D-50937 Cologne, Germany*

³*Department of Condensed Matter Physics, Weizmann Institute of Science, Rehovot 7610001, Israel and*

⁴*Department of Physics, University of California, Berkeley, California 94720, USA*

DERIVATION OF THE COMPACT KPZ EQUATION (CKPZ) AND ITS EFFECTIVE 2D STATIC MODEL

Here we provide some details on the derivation of the compact KPZ equation in one spatial dimension, and the equivalent equilibrium description in terms of an effective Hamiltonian.

Compact KPZ equation

Mathematically, the compactness of the phase field can be formulated as a “discrete” local gauge symmetry of the SCGLE in the amplitude-phase representation of the field $\psi(x, t) \equiv \rho(x, t)e^{i\theta(x, t)}$. Namely, if $\rho(x, t)e^{i\theta(x, t)}$ is a solution of the SCGLE, then $\rho(x, t)e^{i[\theta(x, t)+2\pi n(x, t)]}$ is also a solution, where $n(x, t)$ is an integer valued function. This symmetry reflects the simple physical requirement that any choice of the space-time local definition $\theta(x, t)$ by shifting $2\pi n(x, t)$ must not change the physical results. Therefore, it is crucial to require the effective description to respect this symmetry.

The discrete nature of the gauge transformation indicates that both the temporal and spatial derivative of the phase field have to be taken with care when one tries to derive the dynamical equation for the phase field from the SCGLE. This is due to the fact that the existence of the derivatives for any physical solution of the phase field is not always guaranteed. To see this point, let us consider a solution of the SCGLE, $\psi(x, t) = \rho(x, t)e^{i\theta(x, t)}$ with $\theta(x, t)$ having well defined $\partial_t\theta$ and $\partial_x\theta$ at any space-time point. For a generic gauge transformed solution

$\tilde{\psi} = \rho(x, t)e^{i\tilde{\theta}(x, t)}$ with $\tilde{\theta}(x, t) = \theta(x, t) + 2\pi n(x, t)$, one immediately sees that $\partial_t\tilde{\theta}$ or $\partial_x\tilde{\theta}$ is not well defined if around a certain space-time point, say (x', t') , $n(x', t' + 0^+) \neq n(x', t' - 0^-)$ or $n(x' + 0^+, t') \neq n(x' + 0^-, t')$. Nevertheless, due to fact that the exponential function $e^{i\alpha}$ is a smooth function with respect to α for any physical solution of the phase field, one can always choose a gauge $n(x, t)$ in such a way that *either* the temporal *or* the spatial derivative of the transformed phase field exists everywhere in the space-time domain under consideration, but *not* both.

In the following, we choose the gauge in which the temporal derivative of the phase field exists everywhere. We choose the value of $n(x, t + 0^+)$ according to $\theta(x, t)$ in such a way that $\theta(x, t + 0^+) - \theta(x, t)$ is infinitesimal. Then, the spatial derivative of the phase field is not well-defined everywhere. At the price of introducing a short distance scale, we can circumvent this issue by first rewriting the SCGLE on a discrete 1D lattice with lattice spacing Δ_x , such that the second order spatial derivative is replaced by the a second order finite difference. The discretized SCGLE reads

$$\partial_t\psi_i = (r + u|\psi_i|^2)\psi_i + \frac{K}{\Delta_x^2}(\psi_{i+1} + \psi_{i-1} - 2\psi_i) + \zeta_i, \quad (\text{S-1})$$

with $\psi_i(t) \equiv \psi(i\Delta_x, t)$ and $\langle \zeta_i(t)\zeta_{i'}(t') \rangle = 2\sigma\delta(t - t')\delta_{ii'}/\Delta_x$.

The rest of the derivation goes along the lines of the similar derivation presented in [1]. Plugging the amplitude-phase decomposition of ψ , i.e. $\psi_i(t) = (M_0 + \chi_i(t))e^{i\theta_i(t)}$ with M_0 the homogeneous mean-field solution, into (S-1), we arrive at a coupled discretized equation of motion (EOM) of amplitude and phase fluctuations,

$$\partial_t\chi_i = (r_d - u_d[M_0 + \chi_i]^2)[M_0 + \chi_i] \quad (\text{S-2})$$

$$+ \frac{K_d}{\Delta_x^2}([M_0 + \chi_{i+1}]\cos(\theta_{i+1} - \theta_i) + [M_0 + \chi_{i-1}]\cos(\theta_{i-1} - \theta_i) - 2[M_0 + \chi_i]) \\ - \frac{K_c}{\Delta_x^2}([M_0 + \chi_{i+1}]\sin(\theta_{i+1} - \theta_i) + [M_0 + \chi_{i-1}]\sin(\theta_{i-1} - \theta_i)) + \text{Re}[\zeta_i e^{-i\theta_i}],$$

$$\partial_t\theta_i = (r_c - u_c[M_0 + \chi_i]^2) \quad (\text{S-3})$$

$$+ \frac{K_c}{\Delta_x^2}\left(\frac{[M_0 + \chi_{i+1}]}{[M_0 + \chi_i]}\cos(\theta_{i+1} - \theta_i) + \frac{[M_0 + \chi_{i-1}]}{[M_0 + \chi_i]}\cos(\theta_{i-1} - \theta_i) - 2\right) \\ + \frac{K_d}{\Delta_x^2}\left(\frac{[M_0 + \chi_{i+1}]}{[M_0 + \chi_i]}\sin(\theta_{i+1} - \theta_i) + \frac{[M_0 + \chi_{i-1}]}{[M_0 + \chi_i]}\sin(\theta_{i-1} - \theta_i)\right) + \frac{\text{Im}[\zeta_i e^{-i\theta_i}]}{M_0 + \chi_i}.$$

We linearize in χ and eliminate it adiabatically, made possible since its evolution is fast compared to the gapless phase degree of freedom. From the EOM of χ_i we get

$$\begin{aligned} \chi_i = -\frac{1}{2u_d M_0^2} & \left\{ -\frac{K_d}{\Delta_x^2} ([M_0 + \chi_{i+1}] \cos(\theta_{i+1} - \theta_i) + [M_0 + \chi_{i-1}] \cos(\theta_{i-1} - \theta_i) - 2[M_0 + \chi_i]) \right. \\ & \left. + \frac{K_c}{\Delta_x^2} ([M_0 + \chi_{i+1}] \sin(\theta_{i+1} - \theta_i) + [M_0 + \chi_{i-1}] \sin(\theta_{i-1} - \theta_i)) - \text{Re}[\zeta_i e^{-i\theta_i}] \right\}. \end{aligned} \quad (\text{S-4})$$

Plugging the above equation into the EOM of θ_i , neglecting sub-leading and non-linear amplitude fluctuations $\partial_t \chi_i, \chi_i^2, \chi_i^3$ also here, and keeping only the additive part of the noise, we get the compact KPZ equation

$$\partial_t \theta_i = \sum_{j=i\pm 1} \left[-\bar{D} \sin(\theta_i - \theta_j) + \bar{\lambda} \sin^2\left(\frac{\theta_i - \theta_j}{2}\right) \right] + \bar{\xi}_i, \quad (\text{S-5})$$

with $\theta_i(t) \equiv \theta(i\Delta_x, t)$, $\bar{\xi}_i(t)$ being Gaussian white noise with $\langle \bar{\xi}_i(t) \bar{\xi}_{i'}(t') \rangle = 2\bar{\sigma}_{\text{KPZ}} \delta(t - t') \delta_{ii'}$, $\bar{D} = D/\Delta_x^2$, $\bar{\lambda} = \lambda/\Delta_x^2$, $\bar{\sigma}_{\text{KPZ}} = \sigma_{\text{KPZ}}/\Delta_x$, where

$$D = \frac{u_c K_c}{u_d} + K_d, \quad \lambda = 2 \left(\frac{u_c K_d}{u_d} - K_c \right), \quad \sigma_{\text{KPZ}} = \sigma \frac{u_c^2 + u_d^2}{2r_d u_d}. \quad (\text{S-6})$$

2D static phase model $\mathcal{H}[\theta]$

Here, we construct the effective 2D static equilibrium model for the compact KPZ equation. Conceptually, the idea is to interpret the compact KPZ equation as a mapping from the set of stochastic variables $\bar{\xi}(t) = \{\bar{\xi}_i(t)\}$ with Gaussian path probability distribution

$$\mathcal{P}[\bar{\xi}] \propto e^{-\frac{1}{4\bar{\sigma}_{\text{KPZ}}} \sum_i \int_{t_0}^{t_1} dt \bar{\xi}_i(t)^2} \quad (\text{S-7})$$

to new stochastic variables $\theta(t) = \{\theta_i(t)\}$. The distribution of the new variables can be obtained using the usual relation [2]

$$\mathcal{P}[\bar{\xi}] \mathcal{D}[\bar{\xi}] = \mathcal{P}_\theta[\theta] \mathcal{D}[\theta], \quad (\text{S-8})$$

where $\mathcal{D}[\theta] = \prod_i \mathcal{D}[\theta_i]$ is the functional measure. This yields

$$\mathcal{P}_\theta[\theta] = \mathcal{P}[\bar{\xi}] \left| \frac{\mathcal{D}[\bar{\xi}]}{\mathcal{D}[\theta]} \right| \propto e^{-\mathcal{H}[\theta]/T}, \quad (\text{S-9})$$

where $T \equiv 4\bar{\sigma}_{\text{KPZ}}$ is the effective temperature and $\mathcal{H}[\theta]$ assumes the form

$$\mathcal{H}[\theta] = \int_{t_0}^{t_1} dt \Delta_x \sum_i \left[\partial_t \theta_i + \sum_{j=i\pm 1} \left(\bar{D} \sin(\theta_i - \theta_j) - \bar{\lambda} \sin^2\left(\frac{\theta_i - \theta_j}{2}\right) \right) \right]^2. \quad (\text{S-10})$$

In deriving \mathcal{P}_θ , we used that the Jacobian determinant associated with the change of variables from $\bar{\xi}$ to θ is equal to unity for a retarded regularization of the time derivative in the compact KPZ equation. In the continuum limit, $\mathcal{H}[\theta]$ reduces to the form shown in the main text. Finally, calculating the normalization of \mathcal{P}_θ corresponds to calculating the partition function Z of the model defined by Eq. (S-10) at temperature T ,

$$Z = \int \prod_i \mathcal{D}[\theta_i] e^{-\mathcal{H}[\theta]/T}. \quad (\text{S-11})$$

CROSSOVER BEHAVIOR IN THE TEMPORAL CORRELATION FUNCTION

A crossover behavior similar to the one seen in the temporal phase fluctuation $\Delta_\theta(t_1 - t_2)$ is also observed in the modulus of the condensate temporal auto correlation function

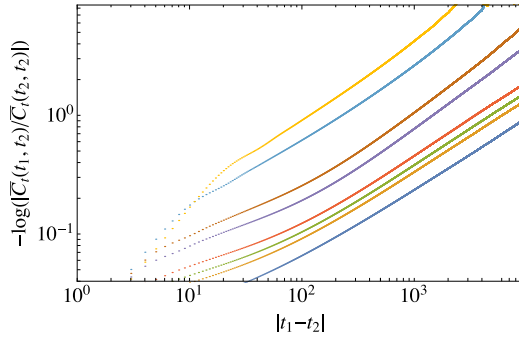


Figure S1. (Color online) The dependence of $-\log(|\bar{C}_t(t_1, t_2)| / |\bar{C}_t(t_2, t_2)|)$ on $|t_1 - t_2|$ for 8 different sets of parameters in the SCGLE at linear system size $L = 2^{10}$. $N_{\text{Traj}} = 10^3$ stochastic trajectories are used to perform the ensemble average. From right to left, the different curves corresponds to $\sigma = 20^{-1}, 12^{-1}, 10^{-1}, 8^{-1}, 5^{-1}, 4^{-1}, 2^{-1}, 1$. Other parameter are $K_d = r_d = u_d = 1, -r_c = u_c = 0.1$, and $K_c = 3$.

$$C_t^\psi(x; t_1, t_2) \equiv \langle \psi^*(x, t_1) \psi(x, t_2) \rangle. \quad (\text{S-12})$$

In practice, by assuming spatial translational invariance of the correlation function, we calculate the spatially averaged correlation functions, i.e., $\bar{C}_t(t_1, t_2) \equiv L^{-1} \int_0^L dx C_t^\psi(x; t_1, t_2)$, which is equivalent to the corresponding correlation function above but helps to reduce the statistical error.

In Fig. S1, at linear system size $L = 2^{10}$, the dependence of $-\log(|\bar{C}_t(t_1, t_2)| / |\bar{C}_t(t_2, t_2)|)$ on $|t_1 - t_2|$ for 8 different sets of parameters in the SCGLE are shown on a the double-logarithmic scale. The exponent β for different parameter choices is extracted from the slope of a selected portion of the corresponding curve of $-\log(|\bar{C}_t(t_1, t_2)| / |\bar{C}_t(t_2, t_2)|)$ on the double-logarithmic scale (cf. Fig. S1). For the noise levels $\sigma = 20^{-1}, 12^{-1}, 10^{-1}, 8^{-1}, 5^{-1}$, the corresponding slopes are extracted by performing linear fits to the data points with $|t_1 - t_2| \in [10^3, 10^4]$. This gives rise to $2\beta = 0.61$, for all the first four curves from below with $\sigma = 20^{-1}, 12^{-1}, 10^{-1}, 8^{-1}$, respectively, where we notice the typical KPZ scaling behavior, but no crossover effect to the anticipated exponential decay. This due to the fact that the crossover time scales corresponding to these noise levels are much larger than the time range available in our simulations.

For the fifth curve from below with $\sigma = 5^{-1}$, one notices a considerably increased slope at the right end of the curve, clearly indicating the crossover effect which sets in within $|t_1 - t_2| \in [10^3, 10^4]$. This is reflected in the extracted exponent with $2\beta = 0.74$. The anticipated exponential decay is expected to manifest itself at even larger $|t_1 - t_2|$, which is however not accessible for our current computation resources.

For the first three curves from above with $\sigma = 1, 2^{-1}, 4^{-1}$, since the local gradient of the curve changing noticeably up to the last accessible data point with the largest value of $|t_1 - t_2|$, denoted as Δt_{max} , the corresponding slopes are extracted by performing linear fits to the data points of a short segment of the curve with $|t_1 - t_2| \in [\Delta t_{\text{max}} e^{-1/4}, \Delta t_{\text{max}}]$ for $\sigma = 4^{-1}, 2^{-1}$, and an even shorter segment of the curve with $|t_1 - t_2| \in [\Delta t_{\text{max}} e^{-1/5}, \Delta t_{\text{max}}]$, for $\sigma = 1$. This gives rise to $2\beta = 1.0$ for all the three curves, which clearly indicates the anticipated exponential decay. However, to further numerically verify this exponential decay in a larger time range is beyond our currently accessible computation resources.

[1] E. Altman, L. M. Sieberer, L. Chen, S. Diehl, and J. Toner, Phys. Rev. X **5**, 011017 (2015).
[2] R. Graham, Springer Tracts in Modern Physics **66**, (Springer, Berlin-Heidelberg-New York, 1973).